INVESTIGATION OF SINTERING DENSITY, COMPRESSIVE STRENGTH AND TRIBOLOGICAL CHARACTERIZATION OF ELECTROLYTIC IRON-ZINC STEARATE COMPOSITE MANUFACTURED BY POWDER METALLURGY PROCESS

S. Kumar[1*] and D.K. Patel[1]

[1]Department of Mechanical Engineering,
IIMT Engineering College,
Meerut, India

Corresponding Author's Email: Sachin.dubey765@gmail.com

Article History: Received 30 July 2025; Revised 08 September 2025; Accepted 29 December 2025

ABSTRACT: Powder metallurgy (PM) provides an efficient method for producing complex metallic components through controlled compaction and sintering. This study examines electrolytic iron powder with zinc stearate (ZnSt) as a lubricant to evaluate the influence of processing parameters on densification and mechanical performance. The experimental variables included compaction load (400, 450, and 500 kN), lubricant content (0%, 1%, and 2%), and particle size ranges (250–300 mesh and 300–350 mesh). Pre-sintering was conducted at 600 °C, and microstructural characterization was carried out using scanning electron microscopy (SEM) and energy-dispersive spectroscopy (EDS). Powders with a mesh size of 300–350 and crushed at 500 kN had the highest density. At 500 kN, the density increased by 18%. The optimum combination of the parameters 300–350 mesh particle size, 2% lubricant, and 500N load was determined to have an optimal density (ϱ) of 6.812 g/cm^3.

KEYWORDS: *Powder metallurgy; Ccompressive strength; Zn stearate; Eelectrolytic Iron Powder; Lubricant*

1.0 INTRODUCTION

The needs of Fe-based soft magnetic materials are required to meet the demands of the electrification process worldwide. Compared to other materials like cobalt and nickel Fe based soft magnetic materials exhibit better magnetic as well as mechanical properties. These materials are used in high frequency transformer magnetic cores, inverters, and high efficiency motor frequency converters [1- 4]. In powder metallurgy (PM) processes the lubricants play a major role in achieving high performance materials. For solid lubricant a thin film is required to be generated in between contact surfaces of the powder particles. After establishing thin film in between the contact surfaces, sliding occurs either between the films or between the film and the substrate. The film formed on powder depends on roughness of the surfaces, the film adherence to the substrate, and the lubricating powder's sintering properties. In sintering process, the loose solid powder stick with the solid substance due to applied compressive force. Lubricants used in to the

mixtures minimize the friction between powder particles. The lubricant works till the temperature of the mixture is below the melting temperature of the lubricant. Kumar et al. [5] fabricated composite composed of atomized iron particles with mesh sizes of 100-200 and 200-300. Three distinct weight percentages of zinc stearate were used: 2.5 weight percent, 5 weight percent, and 7.5 weight percent. There were three different compaction loads: 160 N, 180 N, and 200 N. The sintering temperature was 500 ^{o}C. The result reveals that the particle size influenced significantly to the density of the composite materials. The maximum compression strength was seen for particle size 100-200. Korim et al. [6] investigated the density of Cu–15Fe alloy by adding stearic acid (SA) as a lubricant by powder metallurgy process. The cold compaction pressures used were 50 MPa, 200 MPa, and 350 MPa. The samples were sintered at 1050 °C for 60 min in vacuum. The findings show that the density rose noticeably from pressure 50 MPa to 200 MPa. The alloy's green density increased by 13.2% without using lubricant. In contrast, the green densities with the use of stearic acid increased by 8%. The green density of samples without lubrication and by SA lubricant rose by 13.2 % in the pressure range of 200 MPa to 350 MPa. On the other hand, in the pressure range of 50 MPa to 200 MPa, the sintered density of SA sample rose by 8%. The bending strength and the green density increase with increase in impact velocity. This result can be obtained by the use of pure atomized iron powder. Zinc stearate ranging from 0 weight percent to 2.0 weight percent was used by Yang et al. [7] to create magnetic composites. The composite made by using 2 wt.% zinc stearate created 53.6 nm thin layer of iron phosphate, zinc oxide, and silicon oxide at an annealing temperature of 560 °C. With a low core loss of 174 kW/m^3 and a high permeability of 66.7, this layer offered exceptional soft magnetic properties. The inclusion of lubricant influences hysteresis loss in the overall energy loss of magnetic material Dong et al. [8] examined the behaviour of Znst by mixing in sodium 4- [(4 chlorobenzoyl) amino] benzoate (SCAB) to create the SCAB-Znst composite. Znst was also utilised to lubricate the PP matrix and enhance the dispersion characteristics of SCAB. The outcome showed that the crystallization properties of PP were enhanced and that Znst demonstrates internal lubricating in PP. Znst has a lubricating effect that improves the crystalline and mechanical properties of PP while promoting the dispersion of SCAB in the PP matrix. The flexural strengths and tensile strength of PP/SCAB-Znst was found maximum 40.6 MPa and 42.9 MPa in these combinations. The Znst increased dispersion of SCAB in the PP matrix while also having a lubricating effect, allowing PP's mechanical and crystalline qualities to be improved. Hanejko et al. [9] used a lubricant contained a metal stearate and two waxes with varying melting points such as carnauba wax and Montan wax. When the ANCORMAX 200 lubricant was used at 121 ^{o}C, the density increased from 7.40 g/cm^3 to 7.50 g/cm^3, although the pressure applied was only 10% greater.

The most common lubricants used in traditional cold-compaction procedures are magnesium (Mg), calcium (Ca), and zinc stearates. These lubricants, however, have a lower glass transition temperature. As a result, when heated to 100–150 °C, the combined powder becomes less fluid. For this reason, a new kind of lubricant should be employed throughout the warm compaction process to guarantee that the powder has a homogeneous bulk density and good fluidity [6, 10-14].

This research paper investigates the influence of zinc stearate content weight %, compaction load, and powder particle size of electrolytic iron powder on the properties

ISSN 2180-1053 e-ISSN 2289-8123 Vol.17 No.2

of composite materials. In addition, SEM and EDS analyses were employed to examine the structural features of the materials.

2.0 METHODOLOGY

2.1 Selection of Materials

For fabrication of samples, electrolytic iron powder of two different particles sizes i.e. 250-300 mesh and 300 - 350 mesh were selected. Two particle sizes are sufficient to capture the effect of that factor, while three levels for other parameters are used to detect nonlinear trends.

Table 1: Physical characteristics of electrolytic iron powder

Electrolytic iron powder				**Zinc Stearate**	
Physical characteristic	Value	Chemical Element	Quantity	Chemical Element	Quantity
Size of particles used	250 mesh to 300 mesh and 300 mesh to 350 mesh	Insoluble in HCl	0.0 5%	Chloride (Cl)	0.025 %
Atomic weight	55.85	Arsenic (As)	0.000 5%	Sulphate (SO_4)	0.6 %
Colour	A fine blackish powder	Copper (Cu)	0.00 5%	Heavy metals (Pb)	0.001 %
Purity	99.5 %	Manganese (Mn)	0.05 %	Arsenic (As)	0.0002 %
Bulk Density	2.05 g/cm^3	Sulphide (S)	0.02 %		
		Nickel (Ni)	0.05 %		
		Lead (Pb)	0.00 2%		
		Zinc (Zn)	0.01 %		

The powder was procured from Molychem, Mumbai and Nanopartech Chandigarh. Zinc stearate was taken as lubricant to mix-up in the electrolytic iron powder. Electrolytic iron powder as shown in Fig. 1(a) was used for the preparation of samples. Electrolytic iron powders in two distinct mesh sizes (250–300 and 300–350 mesh) were used. The SEM images of electrolytic iron powder with 250–300 mesh and 300–350 mesh is displayed in Fig. 1 (c) and Fig. 1(d), respectively. The powders had acicular and irregular forms. Particles with a size of 300–350 mesh are smaller than those with a size of 250–300 mesh.

The graphite powder as shown in Fig. 1(b) was used to lubricate the die walls so that composite samples could be removed from them with ease. The experiments were performed on set-up given in Fig. 2 with different combinations of input parameters. Compaction method was used to shape the powder by pressing the punch in the die as shown in Fig. 2(a).

The compaction of powder was carried out according to the standards of MPIF 35 (Metal powder industries federation).

ISSN 2180-1053 e-ISSN 2289-8123 Vol.17 No.2

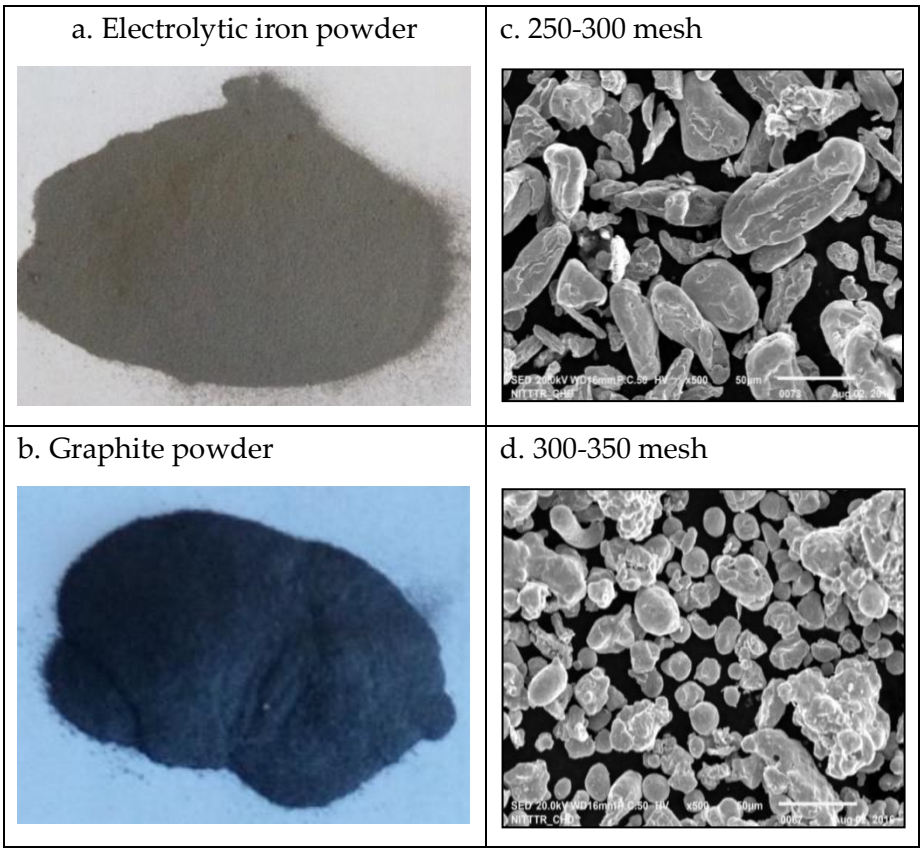

Figure 1: (a) Electrolytic iron powder (b) graphite powder and SEM image of electrolytic iron powder having (c) 250 - 300 mesh (b) 300-350 mesh

The hardened high Cr steel was taken as die material for cold compaction of the composites (Fig. 2b). A blender as shown in Fig. 2 (b) was used to mix the powders.

2.2 Experimental Set-Up

The compaction machine was electrically driven with load capacity of 3000 kN. In compaction 400 kN, 450 kNn and 500 kN loads were used. A funnel is used to feed blended powders into the die cavity to prevent the spreading of powders along the wall area. The cylindrical samples of different compositions (20 mm diameter and 21±2 mm length) were made through the use of die.

2.3 Selection of Process Parameters

The powder size, lubricant and compaction load are the important parameters the affect the properties of the components. The input parameters and their values at different levels are given in Table 2.

ISSN 2180-1053 e-ISSN 2289-8123 Vol.17 No.2

Figure 2: Experimental setup of powder metallurgy process (a) Compaction machine (b) Blender (c) die used in making the samples

Table 2: Input parameters and their values at different levels

Process parameter	Symbol	Level and values		
		1	2	3
Powder Size(mesh)	A	250-300	300-350	-
Lubricant (wt.%)	B	0	1	2
Compaction Load (kN)	C	400	450	500

2.4 Design of experiment

Experiments were conducted on the basis of the Taguchi method to categorize the experimentation into three levels for powder metallurgy process. The L18 Orthogonal array (OA) was used for the experimental work. The opted design level helps in simultaneously analysis of 1 factor at two levels and two factors at three levels.

2.5 Experimentation

The experiments were performed on the powder compaction set-up. Experiments were carried out at two values of powder size, i.e. 250-300 and 300-350. Whereas, three levels of lubricant and compaction load were taken. A total of 18 experiments were carried out. In the experiment the materials were mixed in blender at 200 rpm for 5 minutes in order to have homogenous mixing [15]. The prepared materials were compressed in the die at different loads. The samples were tested on universal testing machine for compressive strength. The Samples were presintered at 600 ^{0}C. Presintering reduces the formation of pores and voids due to trapped lubricant allowing powders to consolidate better. Minimizing residual lubricant helps in maintaining structural integrity and maintaining compressive strength. As Zinc stearate has Mp: 130 °C that evaporates easily at sintering temperature.

3.0 RESULTS & DISCUSSION

The volume of the samples and a specified mass weighted before the manufacturing samples were used to compute the density of the prepared samples. Mass was divided by volume to determine the density value. Each sample's density values are shown in Table 3.

Table 3: Densities of different samples prepared at pre-sintered temperature

Sample number	Mass (g)	Length (cm)	Volume ($cm^{3)}$	Density (g/cm^3)	Sample number	Mass (g)	Length (cm)	Volume ($cm^{3)}$	Density (g/cm^3)
S-1	40	2.204	6.920	5.779	S-10	40	2.205	6.923	5.777
S-2	40	2.014	6.323	6.326	S-11	40	2.016	6.330	6.318
S-3	40	1.914	6.009	6.656	S-12	40	1.910	5.997	6.670
S-4	40.4	2.214	6.951	5.811	S-13	40.4	2.209	6.936	5.824
S-5	40.4	2.004	6.292	6.420	S-14	40.4	2.003	6.289	6.423
S-6	40.4	1.909	5.994	6.739	S-15	40.4	1.909	5.994	6.740
S-7	40.8	2.218	6.964	5.858	S-16	40.8	2.219	6.967	5.856
S-8	40.8	2.003	6.289	6.487	S-17	40.8	2.005	6.295	6.481
S-9	40.8	1.904	5.978	6.824	S-18	40.8	1.903	5.975	6.828

3.1 Calculation of S/N ratios

The mean compressive strength and density values obtained for each sample along with their S/N ratio are shown in Table 3.

Table 4: S/N ratios values for strength and density

Sample number	Powder particle size (mesh)	Lubricant (wt. %)	Compaction load (kN)	Compressive strength (N/mm^2)	Signal to noise Ratio	Density (g/cm^3)	Signal to noise Ratio
S-1	250-300	0%	400	91.31	39.2104	5.779	15.237
S-2	250-300	0%	450	105.28	40.4469	6.326	16.0226
S-3	250-300	0%	500	129.28	42.2306	6.656	16.4643
S-4	250-300	1%	400	128.35	42.1679	5.811	15.2850
S-5	250-300	1 %	450	142.35	43.0671	6.420	16.1507
S-6	250-300	1%	500	168.36	44.5248	6.739	16.5719
S-7	250-300	2%	400	144.23	43.1811	5.858	15.3550
S-8	250-300	2%	450	155.63	43.8419	6.487	16.2409
S-9	250-300	2%	500	169.01	44.5582	6.824	16.6808
S-10	300-350	0%	400	99.10	39.9215	5.777	15.2340
S-11	300-350	0%	450	102.25	40.1933	6.318	16.0116
S-12	300-350	0%	500	140.03	42.9244	6.670	16.4825
S-13	300-350	1%	400	102.23	40.1916	5.824	15.3044
S-14	300-350	1%	450	176.95	44.9570	6.423	16.1548

S-15	300-350	1%	500	206.87	46.3140	6.740	16.5732
S-16	300-350	2%	400	178.23	45.0196	5.856	15.3520
S-17	300-350	2%	450	211.96	46.5251	6.481	16.2328
S-18	300-350	2%	500	238.70	47.5570	6.828	16.6859

3.2 Level mean response analysis

The trend of the quality attributes in relation to the input parameter fluctuation can be analysed with the aid of the level mean response S/N ratios. The density and strength are optimised using the level mean response plots based on the S/N ratios. The delta value was determined for ordering the input parameters. The difference between the greatest and lowest values of S/N ratios was used to calculate the value of delta.

Table 5: Level mean value for S/N ratios of compressive strength and density (Larger is better)

Compressive strength				**Density**			
Level	Powder particle size (A)	Lubricant (B)	Compaction load(C)	Level	Powder particle size (A)	Lubricant (B)	Compaction load(C)
1	42.58	40.82	41.62	1	16.00	15.91	15.29
2	43.73	43.54	43.17	2	16.00	16.01	16.14
3	-	45.11	44.68	3	-	16.09	16.58
Delta	1.15	4.29	3.07	Delta	0.0	0.18	1.28
Rank	3	1	2	Rank	3	2	1

$$\varrho_P = \bar{\rho}_P + (A_0 - \bar{\rho}_P) + (B_0 - \bar{\rho}_P) + (C_0 - \bar{\rho}_P) \quad (1)$$

where $\boldsymbol{\varrho_P}$ is the S/N ratio calculated at the optimum levels and $\boldsymbol{\bar{\rho}_P}$ is the mean S/N ratios of all. Parameters; and A_0 (16.00), B_0 (16.09) and C_0 (16.58) are the S/N ratio values for A, B and C parameters, respectively, at the mean S/N ratio when these parameters are at the optimum density level. The predicted S/N ratio of 16.0022 dB is transformed to ϱ = 6.812 g/cm^3. A compaction load of 500 kN produced the best densification and compressive strength. Finer particles (300–350 mesh) enhanced packing efficiency, leading to higher density. An intermediate zinc stearate content (2 wt.%) provided optimal strength due to effective lubrication during compaction and complete burnout during pre-sintering. Thus, by analyzing level means of S/N ratios, the optimum parameter combination for achieving high density and compressive strength was identified.

3.2.1 Compressive Strength

Fig.3 (a)–(c) displays the level mean response plots for different quality attributes based on the S/N ratios of compressive strength. As can be seen in Figure 1a, a bigger S/N ratio corresponds to a particle size 300–350. The S/N ratio was lower for particle size 250-300.

ISSN 2180-1053 e-ISSN 2289-8123 Vol.17 No.2

The variation of S/N ratios for the lubricant utilised is depicted in Fig.3 (b). It has been observed that the S/N ratio is higher at 2 weight percent of lubricant, which is beneficial for attaining a decent compressive strength. When no lubricant was applied, the S/N ratio was the lowest. The slope of the graph decreases as the lubricant percentage increases in the mixture. Fig.3 (c) shows the graph of S/N ratios for compaction load. Improved compressive strength is indicated by the greater S/N ratio that was found to match to the 500 kN compaction load. The improvement in compressive strength at 500 kN compaction load is evidenced by the higher signal-to-noise (S/N) ratio obtained under this condition. In Taguchi analysis, the S/N ratio is used to quantify the robustness of a response; a higher S/N ratio indicates more consistent and reliable performance with reduced variability. The S/N ratio at the 400 kN was the lowest. It has been concluded that the increase in lubricant, compaction load and grain size enhanced the properties of the samples.

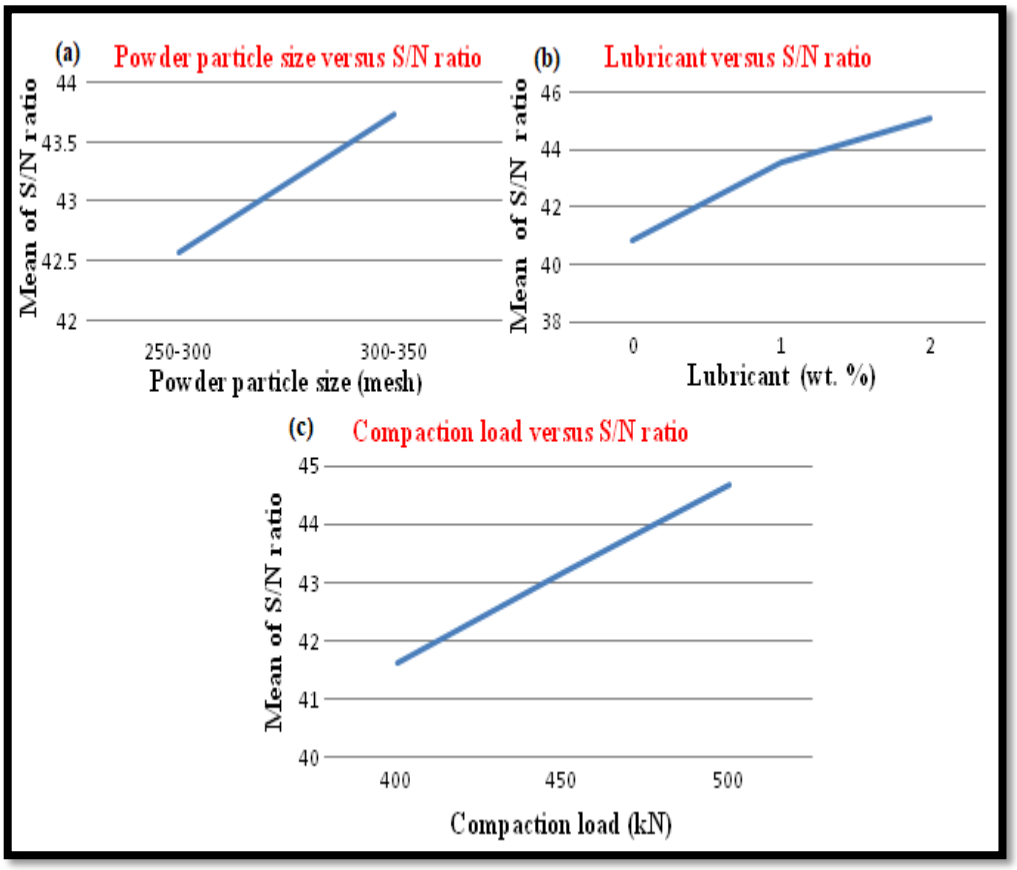

Figure 3: Main effects plot for signal to noise ratio of compressive strength

3.2.2 Density

The S/N ratio corresponding to particle size 250-300 and 300-350 are same as shown in Fig.4 (a) It means the particle size does not affect the density of the composite material. Fig. 4(b) shows the S/N ratio for lubricant used to modify the density of the composite.

ISSN 2180-1053 e-ISSN 2289-8123 Vol.17 No.2

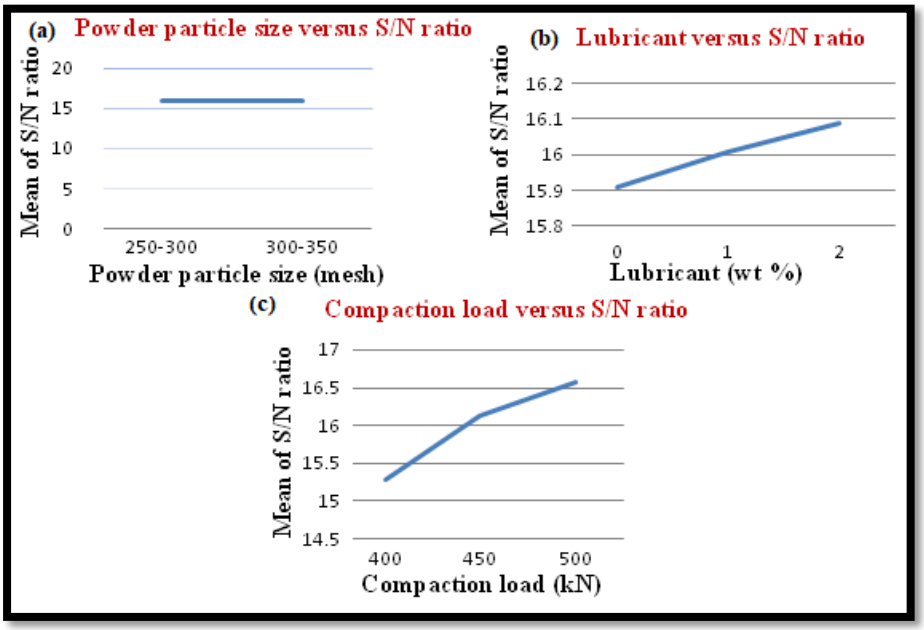

Figure 4: Main Effects plot for signal to noise ratio of density

The S/N ratio corresponding to 2 wt. % of lubricant used is largest, which is desirable for high density. The value of S/N ratio is lowest when lubricant is not used in mixture. Fig.4 (c) depicts the largest density at 500 kN and lowest at 400 kN. The density is larger at higher value of compact load. Smaller particles can fill voids, reducing the initial porosity in the green compacts. This improves powder packing density before sintering. Small particles have large surface area which increases the number of surface atoms with high diffusivity**.** Small changes in particle size during compaction do not significantly alter the packing efficiency of powders, particularly if the powder is already tiny, as in the case of electrolytic iron, which contains irregular and dendritic particles. Smaller particles can help pack by filling up the spaces between bigger ones, although this advantage is diminished in powders that are mono-sized, which is common in laboratory settings. When deciding final density, compaction pressure typically has a greater influence than particle size. Reducing particle size further yields diminishing returns on increasing density after the maximum green density is reached at a particular pressure. Even when density is relatively constant, zinc stearate increases compressive strength by improving sintering kinetics, decreasing flaws, and improving particle contact quality.

3.3 Analysis of variance (ANOVA)

ANOVA is used to find out the percentage contribution of input parameters for the response values.

3.3.1 Compressive Strength

Table 6 depicts the contribution of input parameters by using ANOVA based on S/N ratio with significance level of 0.05 or confidence level of 95%. The lubricant dominates in the composite material with 50.60% contribution. The compaction load contributed 25.75% followed by powder particle size with 8.9%. This investigation confirms that lubrication is a key factor in increasing compressive strength. Zinc stearate reduces die wall friction,

which allows higher effective compaction pressure to be transmitted uniformly into the powder mass. This results in better green strength as well as particle rearrangement.

Table 6: ANOVA data for signal to noise ratio of compressive strength

Source	DOF	Sequential SS	Adjusted SS	Adjusted MS	F	P	% contribution
Powder particle size	1	2750.8	2750.8	2750.84	7.8916	0.014767	8.90
Lubricant	2	15646.6	15646.6	7823.30	22.4434	0.000060	50.6
Compaction Load	1	7946.5	7946.5	7946.45	22.7968	0.00036	25.7
Error	13	4531.5	4531.5	348.58			14.6
Total	17	30875.4					100

3.3.2 Density

Table 7: ANOVA data for signal to noise ratio of density

Source	DOF	Sequential SS	Adjusted SS	Adjusted MS	F	P	% Contribution
Powder particle size	1	0.00002	0.00002	0.00002	0.003	0.957837	0.08
Lubricant	2	0.05449	0.05449	0.02724	4.929	0.025522	2.02
Compaction Load	1	2.56873	2.56873	2.56873	464.735	0.00000	95.3
Error	13	0.07185	0.07185	0.00553			2.6
Total	17	2.69508					100

Table 7 shows the contribution of each input parameter by using ANOVA based on S/N ratio with significance level of 0.05 or confidence level of 95%. The compaction load is found to be dominant factor for density of composite with 95.3% contribution. The Lubricant contributed 2.02% followed by Powder particle size with 0.08 %. During Presintering, Zn Stearate must decompose. At 2 % or higher content, burnout leaves residual carbonaceous species that counteract densification [16] and compaction load play their roll to increase the density.

3.4 Tribological Analysis of Composites.

The microstructure of iron powder is depicted in Fig. 5 and 6, which are SEM pictures of four samples that were examined for this work. A magnification of x 500 was used for the scanning in order to get a clear image of the powder particles. Samples S-4 and S-13 SEM images are displayed in Fig.5.

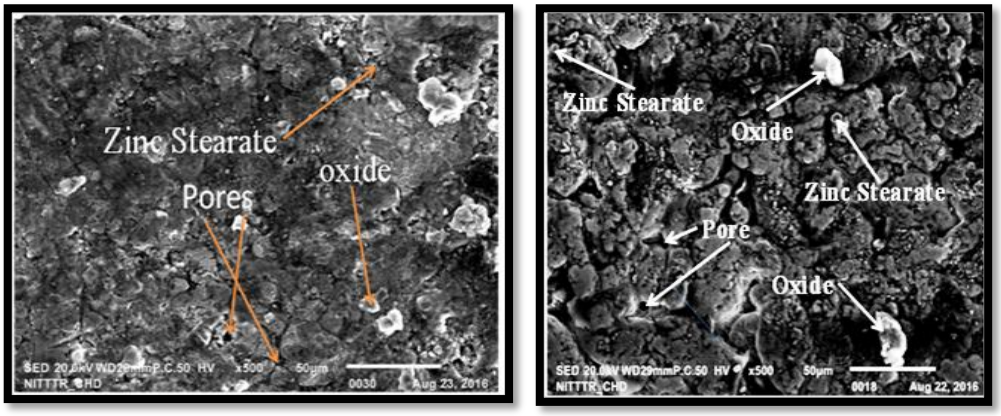

Figure 5: SEM image of sample S-4 and S-13

The distribution of zinc stearate particles in the composites is clearly shown in the SEM image. In the compressed samples, the oxide and pore are formed. The sample's density and compressive strength were determined to be 5.811 g/cm^3 and 128.35 N/mm^2, respectively. Sample S-4's inadequate particle bonding results in poor compaction. Sample-13 had a density of 5.824 g/cm^3 and a compressive strength of 102.23 N/mm^2. According to the SEM image, sample S-13 has more more mores than sample S-4Even the particles of zinc stearate were evenly spaced. Fig. 6 displays the SEM picture of samples S-9 and S-12. Compared to sample S-9, sample S-12 has more pores. Sample S-9 has a density of 6.824 g/cm^3 and a compressive strength of 169.01 N/mm2. In contrast, sample S-12 had a density of 6.670 g/cm3 and a compressive strength of 140.03 N/mm^2. Sample S-9's low porosity gives it greater density and compressive strength. Sample S-9 has 2% lubricant and has highest compressive strength and density among samples discussed. This is because the presence of higher lubrication yields homogeneous distribution of particles and applied load.

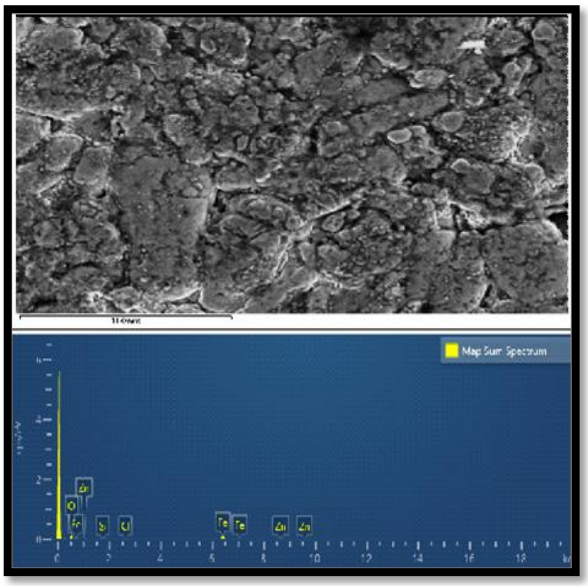

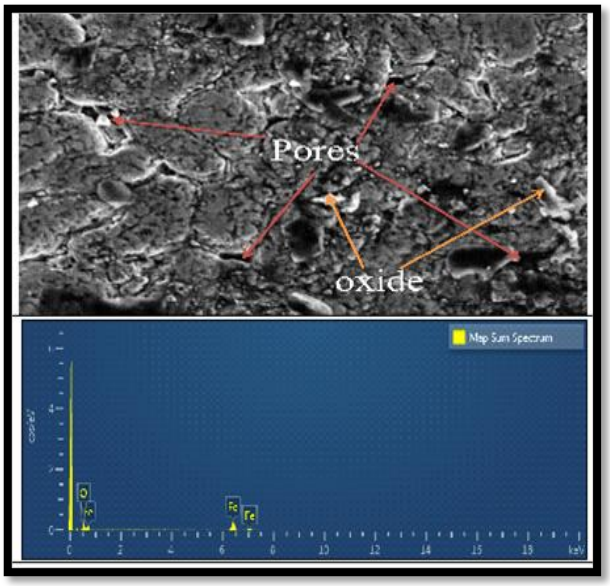

Figure 6: SEM and EDS image of sample S-9 and S-12

As the zinc stearate concentration rises, the fluidity and apparent density of Fe-based powder also rise because the smaller particle size of the powder gave better lubricating effect and reduced arch bridge effect among the powder particles. The amount of pores and the powder interlocking have a significant impact on the strength of the warm compact. Generally, breakout occurs at the section where pores are densely present due to low interlocking between the particles [14]. It is beneficial to accelerate the removal and deformation of powder particles in the warm compaction process because the homogenous lubricating film on the surface of the Fe powder particles that reduces the friction and raise the pressure. Since the warm compaction reduces the yield strength of Fe-based powders as they heat up that raised the powders' deformability and compressibility.

3.5 EDS of Composites

The EDS analysis was carried out in conjunction with SEM to validate the chemical composition and elemental distribution within the composites. The spectra confirmed the successful incorporation of alloying elements and reinforcement phases into the iron matrix. Notably, no traces of undesirable secondary phases such as excessive oxide layers were detected, which supports the absence of interfacial degradation and explains the observed improvement in compressive strength. Furthermore, EDS elemental mapping revealed a uniform dispersion of finer reinforcement particles in samples compacted at 500 kN, correlating with the higher density and S/N ratio obtained under this condition. In contrast, at higher reinforcement contents, localized clustering detected by EDS corresponded with lower mechanical performance due to poor load transfer efficiency. These findings demonstrate that the optimized processing parameters not only improved densification but also promoted chemical and microstructural homogeneity, thereby ensuring enhanced strength and reliability of the developed composites.

In this case, EDS coupled with SEM is utilized to characterize the composite. Two distinct categories-one with and one without lubricant. Samples S-12 and S-9 EDS images are

ISSN 2180-1053 e-ISSN 2289-8123 Vol.17 No.2

displayed in Fig. 6. Zn is present in the composites, as shown by the high peaks.

4.0 CONCLUSION

i. The density and compressive strength of the zinc stearate-added electrolytic iron powder composites were examined in relation to the effects of powder particle size, lubricant quantity, and compaction load. The following is a list of the conclusions reached:
ii. The powder particles' irregular, dendritic, spherical, and flake shapes were found in SEM pictures.
iii. The Sintered density of the composites increases with increasing the compaction load due to better bonding between the powder particles. Finer particle sizes at highest compaction load are well compacted due to irregular and dendritic shape of the particle.
iv. Maximum density was achieved for 300-350 mesh size particles composites. The compaction load dominated the density with 95.3% contribution due to evaporation of lubricant, whereas in compressive strength the lubricant dominated with 50.6% contribution. In density error was found 2.6% whereas in compressive strength the error was 14.6 % which is admissible.
v. The greater S/N at 500 kN suggests the same optimal configuration, and the confirmation means are within the expected confidence interval of the projected response, therefore the 14.6% compressive strength error is in line with the robustness criterion in Taguchi designs
vi. Since the optimisation maintains the ideal factor combination and agrees with the S/N-based robustness, the 2.6% density error inside the instrument and the 14.6% strength error common for sintered, particle-reinforced Al/Fe composites do not invalidate the optimisation.
vii. At compaction load 500 kN, the density increased by 18%.
viii. The optimum combination of the parameters 300–350 mesh particle size, 2% lubricant, and 500N load was determined to have an optimal density (ϱ) of 6.812 g/cm^3.

REFERENCES

[1] S. Vovk, J. Füzer, S. Dobák, P. Kollár, R. Bureš, M. Fáberová & V. Zaspalis, "Soft magnetic composite based on iron in sintered Mn–Zn ferrite matrix without non-magnetic coating". *Ceramics International*, vol. 49, no.18, pp. 30137-30146, 2023.

[2] L. Zhang, Y. Liu, S.U. Rehman, L. Wang, Y. Chen, S. Shen & T. Liang, "In situ synthesis of Fe_3O_4 coated on iron-based magnetic microwave absorbing materials and the influence of oxide magnetic materials on microwave absorption mechanism". *Ceramics International*, vol.49, no.8, pp.12972-12979,2023.

[3] B. V. Neamţu, M. Năsui, G. Stoian, F. Popa, T. F. Marinca, P. Bere, ... & I. Chicinaş. Influence of coating process on the magnetic properties of cold-sintered CoFeSiB@ BaTiO3 fibres based soft magnetic composites. *Ceramics International*, 49(24), 40914-

40923,2023.

[4] G. Liu, B. Dai, Y. Ren, K. Zhang, D. Ye, C. Hu, & S. Fu. "Microstructure and magnetic properties of nickel-zinc ferrite ceramics fabricated by spark plasma sintering". *Ceramics International*, 48(8), 10412-10419, 2022.

[5] R. Kumar, S. C. Vettivel, J. Madan, B. S. Pabla, & S. Kumar. Characterization, "Physical and Mechanical Behavior of Sintered Atomized Iron–Zinc Stearate Composite". *Transactions of the Indian Institute of Metals*, 71, 41-55, 2018.

[6] N. S. Korim, A. Elsayed, & L. Hu. "Impacts of Lubricant Type on the Densification Behavior and Final Powder Compact Properties of Cu–Fe Alloy under Different Compaction Pressures". *Materials*, 15(16), 5750, 2022.

[7] S. Yang, J. Xu, M. Tian, J. Wang, T. Yang, G. Li, & X. Liu. "Microstructure evolution and soft magnetic properties of Fe-based nanocrystalline soft magnetic composites coated with lubricant". *Advanced Powder Technology*, 34(5), 104024, 2023.

[8] Y. Dong, F. Lin, T. Zhao, M. Wang, D. Ning, X. Hao, & B. Wang. "Dispersion and Lubrication of Zinc Stearate in Polypropylene/Sodium 4-[(4-Chlorobenzoyl) Amino] Benzoate Nucleating Agent Composite". *Polymers*, 16(13), 1942, 2024.

[9] F. G. Hanejko & W. Tambussi. U.S. Patent Application No. 15/397,303, 2017.

[10] H. H. Zhang, Z. L. Liu, X. Q. Liu, Z. H. Tang, & D. H. Zou. "Effects of lubricants on the warm compaction process of Fe-based powder metallurgy materials". *Powder Metall Technol*, 35(2), 128, 2017.

[11] C. H. Ye, J. S. Huang, Q. Li, & Z. Wang. "Effects of lubricants on the properties of FeSiAl magnetic powder cores made by warm compaction". *Mater. Sci. Eng. Powder Metall*., 21, 783-788, 2016.

[12] A. Abdallah, M., Habibnejad-Korayem, & D. V. Malakhov. "Are large particles of iron detrimental to properties of powder metallurgy steels?". *Metals*, 10(4), 431, 2020.

[13] A. Shirani, L. A. Perales, & L. Chantal. "Impact Assessment of Lubricants on Powder Properties in Metal Powder Premixes". *Journal of the Japan Society of Powder and Powder Metallurgy*, 72(Supplement), S135-S141, 2025.

[14] M. M. Rahman, S. S. M. Nor, & A. K. Ariffin. "Effect of lubricant content to the properties of Fe-based components formed at above ambient temperature". *Procedia Engineering*, 68, 425-430, 2013.

[15] S. Kumar, S. R. Kumar, S.C. Vettivel. "Tribological behavior of sintered electrolytic iron-zinc stearate added compacts" *Material Science and Engineering technology*, 2023. DOI: 10.1002/mawe.202200251